



SITE CLASSIFICATION BASED ON SPECTRAL AMPLIFICATION PATTERNS FOR MICROTREMOR H/V RATIOS

Víctor Hitiel Rodríguez Sardiña¹ and Saburoh Midorikawa²

SUMMARY

The authors apply soil response estimation techniques employing accelerograms for fifteen earthquakes recorded at the Yokohama Strong Motion Network and its vertical array of nine sites, plus microtremor data recorded at all 150 sites. Assessment of the reliability of surface to a reference site- and horizontal to vertical- spectral ratios of S-waves, Coda, and microtremors, relies on cross-validation with both, surface to borehole spectral ratios, and theoretical soil response functions for vertically incident SH plane waves calculated from the vertical array and logging data, respectively. The results indicate that the H/V of microtremors provides a better match of soil response estimations when considering no more than $\pm 30\%$ mismatch in the determination of the predominant periods. The application of pattern recognition reveals a category structure that fits the mutual relationship of ground motion- and microtremor-based estimations. The calculation of surface to borehole spectral ratios for the vertical components of ground motion and microtremors, as well as the computation of theoretical H/V spectral ratios for SV plane waves confirms the robustness of the grouping scheme. The nine spectral amplification patterns composing the category structure thus validated serve as the cornerstone of our site classification method. The method constitutes an attempt at expanding the applicability of microtremor-based site effects estimations through the improvement of their reliability. To achieve it, we exploit the nexus between the nine amplification patterns and the corresponding local geological conditions revealed in the course of our study. The prospect of obtaining more reliable site effects parameters from a relatively simple analysis at a comparatively low economic cost, combined with the possibility of recording without strict spatial or time restrictions turns microtremors into a particularly appealing approach.

INTRODUCTION

In the course of previous studies [1, 2], the authors had the rather infrequent opportunity of accessing and compiling an extensive amount of earthquake ground motion accelerograms recorded at the 150 sites composing the Yokohama Strong Motion Network illustrated in Fig. 1. Subsequent compilation of microtremor recordings at these 150 sites completed a database that allowed us to apply several of the spectral ratio techniques proposed to estimate the magnitude of local site effects on ground motion using both, microtremor and earthquake ground motion data. Their comparative evaluation indicated that, when

¹ Department of Built Environment, Interdisciplinary Graduate School of Science and Engineering, G3-8f, Tokyo Institute of Technology, 4259, Nagatsuta, Midori-ku, Yokohama, Japan

applied to S-waves (H/V_S), Coda (H/V_C), or microtremor recordings (H/V_M), the horizontal to vertical motion spectral ratios (H/V) provide similar soil transfer functions. At about 30% of the 150 sites under consideration, however, the H/V technique furnishes amplification spectra that do not match those obtained from the application of better understood methodologies, as for instance the surface-to-borehole (H_S/H_B), or the surface-to-reference site (H_S/H_R) techniques [1,2,3]. Notwithstanding, thorough statistical analysis of the mismatching trends and their representative outliers indicates that microtremor-based H/V_M spectra provide more reliable site effects estimations than their S-waves and Coda counterparts. Before proposing concrete guidelines targeting the use of microtremors, however, we considered it necessary to identify the general trends and common features accompanying both success and failure of the H/V_M technique and their relation with the local geological conditions. Accordingly, in this paper we focus on the elucidation of these issues in order to propose a new site classification scheme that targets the improvement of the accuracy and reliability of microtremor-based site effects estimations.

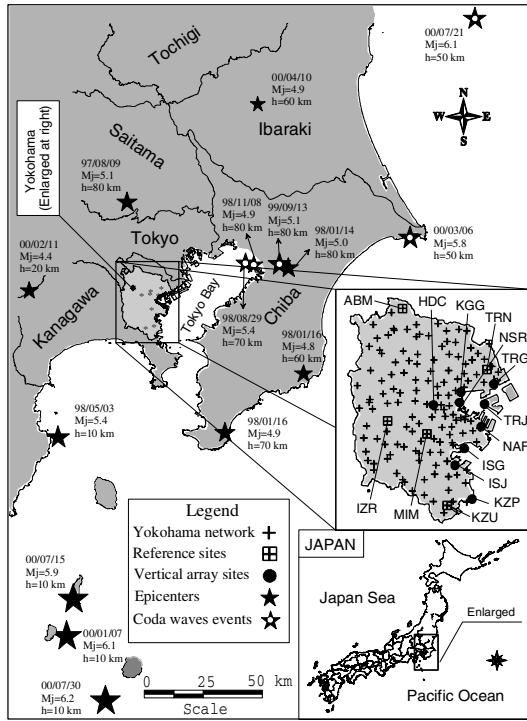


Figure 1. Location of Yokohama City, its strong ground motion network, and epicentres of the events analysed.

APPLICATION OF PATTERN RECOGNITION

Classification involves the process of assigning a new observation to its proper place in an established set of categories. In order to classify, however, we must have previous knowledge of the features or attributes characterising each category. Therefore, before we can successfully evaluate and classify H/V_M -based site effects estimations we need to define a category structure that fits the observed H_S/H_R and H/V_M amplification spectra and their mutual relationship. Obviously, when analysing this relationship, the logarithmic scale of the spectra makes personal judgement even more prone to error and bias. We must also take into consideration that an amount of 290 final amplification spectra makes quite arduous the analysis of the relation between amplification spectra attained from the analysis of ground motion, microtremors, and the logging data. In this regard, we find it worth considering the following issues:

- 1) Surface geology maps display only the distribution of the top layers composing the soil profile. Consequently, the relation between the local geology and the predominant periods turns clear only in the case of resonance frequencies located in the short period part of the spectrum, namely, for resonance layers very close to the surface
- 2) Different soil profiles may certainly appear characterised by similar predominant periods and maximum spectral ratios. Nevertheless, the overall shape of their corresponding amplification spectra may still appear quite contrasting. Thus, reducing the problem to the analysis of peak periods and maximum amplification ratios seems equivalent to restricting the analysis to a very small portion of the whole spectrum

This makes it quite difficult to disentangle the relation between spectral characteristics and logging data. In this context, we took into consideration previous studies suggesting that spectral ratios calculated at different frequencies of the spectrum reflect the characteristics of the soil profile at different depths. Thus seen, each soil layer operates as one of the components of a multi-layered filter acting on the upcoming waves, and accordingly, we can treat the overall shape of the amplification spectra as an indirect representation of the underground structure of the sites. In other words, if by considering their overall shape the amplification spectra happen to cluster into homogeneous groups, then the corresponding S-wave velocity profiles may also share similar characteristics. In order to corroborate the validity of this hypothesis to our particular case, we decided to group the sites taking into consideration, simultaneously, the following factors:

- 1) The shape of the whole H_S/H_R and H/V_M amplification spectra within the frequency range of interest
- 2) The level of coincidence between predominant periods and maximum amplification ratios
- 3) The general agreement level between ground motion and microtremor based estimations

Unfortunately, traditional statistical tools now become ineffective, for they all share a common drawback: they seem limited to the analysis of up to two variables at unison, namely, to bivariate analysis. However, the application of pattern recognition techniques turns into a plausible alternative, for their implementation relies on the utilisation of groups of variables describing the problem under analysis. This opens the possibility of defining relatively homogeneous clusters of amplification spectra, thereby defining their category structure. In our particular case, by applying a hierarchical clustering method to group the sites taking into consideration the factors previously mentioned, we implicitly accept the following assumptions regarding our data set: a) The existence of different levels of matching between ground motion and microtremor based estimations, b) The likelihood of expressing these similarity levels as a similarity measure calculated from our H_S/H_R and H/V_M amplification spectra, and c) The possibility of grouping the sites through the implementation of a clustering scheme using this similarity measure.

We find it worth clarifying that in cluster analysis we can give operational meaning to the term “mutual similarity” but through: 1) The selection of variables representative of the problem under analysis, 2) The implementation of an appropriate equalisation operation, 3) The assignment of a set of weights reflecting our objectives, and 4) The calculation of a similarity measure that serves as the cornerstone of the clustering process. We complied with these precepts by testing different combinations of a variety of similarity measures with different weighing and clustering schemes. The final sequence of operations applied in our study comprised the following stages:

- 1) *Selection of attributes:* As illustrated in Figure 2, we characterised the 145 sites H_S/H_R and H/V_M amplification spectra through twenty-five spectral ratios representing the contribution at different frequencies, from 0.5 to 10 Hz, and the corresponding predominant periods and maximum spectral ratios at each site.

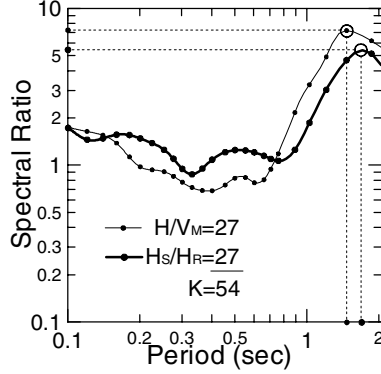


Figure 2. Set of variables employed in the clustering process

2) *Betterment of the data set:* We must consider that processing these variables in raw form may result in misleading results, for they would carry deceptive weights in the similarity coefficient calculations. Accordingly, we normalised the data values to the same unit system, and weighed the spectral ratios in terms of the standard deviation of the corresponding distributions through the following expression:

$$x' = \frac{(x - x_{\min})}{\sigma(x_{\max} - x_{\min})} \quad 1$$

where x stands for the variable to undergo equalisation, x_{\min} and x_{\max} represent the minimum and maximum values of the x distribution, and σ its standard deviation.

3) *Calculation of a similarity measure:* We employed the Euclidean distance dissimilarity coefficient (D), given by the vectorial distance separating two sites i and j within a p dimensional Euclidean space E^p defined by the number of n variables characterising each individual:

$$D_{ij} = \sqrt{\sum_{n=1}^{n=p} (x_{ni} - x_{nj})^2} \quad 2$$

As we employ fifty-four variables, each coefficient represents a distance within a fifty-four dimensional Euclidean space.

4) *Clustering of sites and definition of groups:* We applied the Ward clustering algorithm, and obtained the dendrogram illustrated in Figure 3. This plot illustrates at which similarity levels we can merge the sites into increasingly similar subgroups as we move from top to bottom. Its analysis suggests dividing the dataset into the nine groups of sites indicated with a grey line.

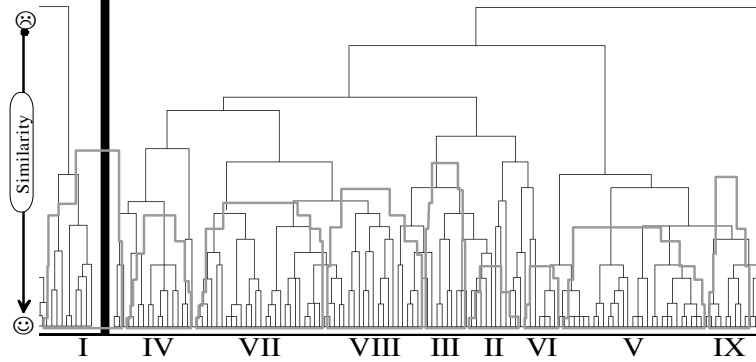


Figure 3. Dendrogram attained from the pattern recognition process. The plot suggests dividing the dataset into the nine groups indicated with the grey lines.

5) *Generalisation into patterns:* It turns impossible to arrive to general conclusions if we do not summarise the results properly. In our case, a proper generalisation must take the form of a category

structure that complies with our objectives and fits our dataset. Accordingly, we calculated the mean H_S/H_R and H/V_M amplification spectra for the nine groups of sites delimited with grey lines in Fig. 3. The process previously described leads to the attainment of what we denominated *Spectral Amplification Patterns (SAP)*, and illustrate in Figure 12. In other words, a spectral amplification pattern (SAP hereafter) represents the general trend common to amplification spectra occurring at sites sharing similar soil profile characteristics. This also implies that, thus defined, a spectral amplification pattern, although within the bounds of an inherent natural variability, appears repeatedly within a certain area.

CORRELATION OF THE SPECTRAL AMPLIFICATION PATTERNS WITH THE LOCAL GEOLOGICAL CONDITIONS

When judging the robustness of our grouping scheme, a logical choice consists in checking the presence or not of a very desirable feature in any category structure, namely, low levels of similarity among patterns, but high levels of similarity between their member sites. The $H/V_M \pm \sigma$ region illustrated in Figure 12 indicates that the nine SAPs do display a relatively stable spectral shape along the whole frequency interval under consideration. When comparing the average H/V_M and H_S/H_R transfer functions characterising different SAPs, however, the contrast among different patterns turns into an apparently differentiating feature. For instance, Pattern I member sites display a conspicuous mismatching trend, quite different form that typical for Pattern IX sites, which show a remarkable coincidence of estimations. This proves the robustness of the SAPs in terms of spectral characteristics.

The next step consists in checking the link between these spectral characteristics and the local geological conditions. Analysis of the soil profiles for the sites composing each pattern confirms that indeed, each SAP appears characterised by S-wave velocity profiles sharing distinctive features. Confronted with the impossibility of plotting all the soil profiles, however, we opted for selecting a soil profile representative of the general trend typical for each SAP. Figure 4 illustrates these typical S-waves velocity profiles, corresponding to sites whose amplification spectra match the closest the average spectra characterising each particular pattern. At this point, we find it worth providing a general description of the main spectral and S-wave velocity features characterising each pattern:

Pattern I: Seventeen sites characterised by mismatching trends of essentially flat amplification spectra (Fig. 12-I). When compared to the H_S/H_R technique, the H/V_M method provides predominant periods conspicuously shifted toward longer values. As exemplified in Fig. 4a, the soil profiles present frequent intercalations of sandy deposits causing recurrent changes in the S-wave velocities. Conversely, this leads to an overall low impedance level between lower and upper strata.

Pattern II: Eight sites characterised by essentially flat amplification spectra, with values plotting around two. Nevertheless, the H_S/H_R and H/V_M predominant periods show good agreement (Fig. 12-II). The S-wave velocity profiles display a moderate contrast between the lower strata and a thin package of sediments on top, usually not exceeding about five metres (Fig. 12b). Seismic engineers often classify these sites as rock, or soft rock sites.

Pattern III: Eight sites characterised by semiflat H/V_M , coincident amplification spectra with a trend resembling that of Pattern II sites. The H_S/H_R transfer functions, however, display apparently larger amplification ratios toward the short period part of the spectrum. The S-wave velocity profiles display gradual increments resulting in a stair-like S-wave velocity pattern as we move downward (Fig. 4c). Relatively low impedance level between lower strata and upper sediments with a thickness varying between five and fifteen metres.

Pattern IV: Thirty sites displaying semiflat, coincident spectral shapes (Fig. 12-IV). The soil profiles display a moderately good impedance level between lower strata and upper sedimentary packages with a thickness of about ten metres. The S-wave velocity profiles often display an attenuated version of the stair-like pattern typical of Pattern III sites (Fig. 4d).

Pattern V: Twenty-seven sites exhibiting semisharp, coincident spectral shapes (Fig. 12-V). The soil profiles display a relatively good contrast between underlying strata and upper sediments, in this case thicker than those for Pattern IV sites, as a rule with a width varying between fifteen and twenty metres (Fig. 4e).

Pattern VI: Fourteen sites displaying semisharp, coincident H/V_M spectral shapes. The H_S/H_R spectra, however, display smaller maximum amplification ratios (Fig. 12-VI). Soil profiles characterised by good contrast between lower strata and upper sediments approximately twenty metres thick (Fig. 4f).

Pattern VII: Twenty sites exhibiting sharp, coincident spectral shapes (Fig. 12-VII). Soil profiles characterised by very good contrast between underlying layers and sedimentary packages about twenty metres thick. The S-wave velocity profiles appear to resemble those typical of Pattern VI sites, but now with either thicker sediments or higher impedance levels.

Pattern VIII: Nine sites characterised by sharp, coincident spectral shapes (Fig 12-VIII). The S-wave velocity profiles display a very good contrast between lower strata and upper sedimentary packages with a thickness of about thirty metres, mostly free of sudden changes in the S-wave velocities.

Pattern IX: Nine sites characterised by very sharp, coincident spectral shapes (Fig. 12-IX). The soil profiles exhibit a characteristic L-shaped S-wave velocity profiles indicating very good contrast between lower strata and the upper packages of sediments. The thickness of the sedimentary packages exceeds thirty metres, up to sixty metres Fig. 4i).

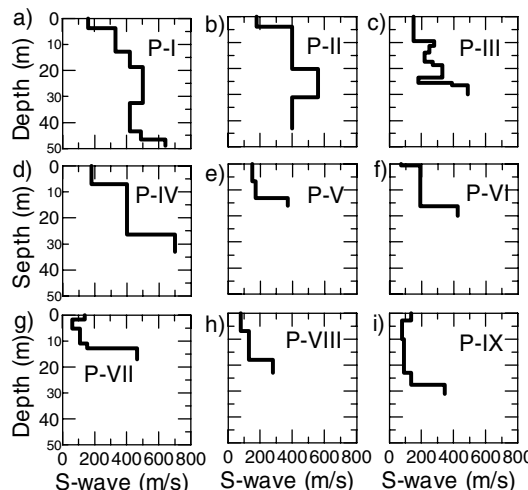


Figure 4. Typical S-wave velocity profiles for the nine SAPs

Thus, examination of the logging data reveals that the sites composing each pattern appear characterised by similar H_S/H_R and H/V_M amplification spectra, as well as by similar velocity profiles and lithological composition of the soil layers. As the pattern recognition leading to the definition of these nine patterns took into consideration only the characteristics of the H_S/H_R - and H/V_M - amplification spectra, these regularities shared by members of the same group implicitly support the following points:

- 1) The appropriateness of the grouping scheme derived from the clustering process
- 2) The spectral amplification patterns reflect the characteristics of the soil profile
- 3) The possibility of linking each spectral amplification pattern to specific soil profiles

VALIDATION OF THE ROBUSTNESS OF THE SPECTRAL AMPLIFICATION PATTERNS USING THE VERTICAL ARRAY DATA

We do count with ground motion data simultaneously recorded at the vertical array sites of the Yokohama Strong motion Network illustrated in Fig. 5. Accordingly, we can employ these data to

calculate the amplification spectra for the vertical components of motion along the frequency interval under analysis. The calculation of surface to borehole spectral ratios for the vertical components of motion relies on a theory similar to that applied to calculate the horizontal motion amplification [1,2,3]. In this case, however, we simply replace the horizontal components of motion by the vertical ones to yield the expression:

$$G_V(f) = V_S(f)/V_B(f) \quad (3)$$

where $G_V(f)$ represents the effect of the soil profile on the vertical components of ground motion along the frequency f , and $V_S(f)$ and $V_B(f)$ denote the vertical motions registered at the surface and at the base engineering rock accelerographs, respectively. We applied Eq. 3 to the fifteen events' accelerographic data registered at the vertical array sites shown in Fig. 5. We illustrate the resulting amplification spectra for the vertical motion with a thin solid line in Fig. 6. Analysis of this figure allows us to state that, as a rule, the vertical component of ground motion does not undergo significant amplifications at periods longer than one second. Furthermore, at sites characterised by relatively simple S-wave velocity profiles, such as NAF, ISJ, and KGG, the vertical components of motion appear mostly free of the effects of the soil profile, except for periods shorter than 0.2 seconds. At the rest of the sites, namely TRG, KZP, HDC, ISG, NSR, and TRJ, the vertical component of motion undergoes amplification at periods shorter than one second. Notwithstanding, at these sites the largest amplifications of the vertical motion appear to take place at periods shorter than 0.2 seconds, and remain within a factor of two for the interval 0.2~1 sec. The results appears to indicate that, except for periods lower than 0.2 sec, the vertical components of motion do not undergo significant amplifications under the influence of the soil profile. This in turn appears to substantiate the use of the vertical components at the surface as representative of the incident waves arriving at the base of the sedimentary packages. Notwithstanding, amplification of the vertical component at different frequencies, although relatively small, will obviously sway the corresponding H/V amplification spectra away from the transfer functions for the horizontal component of motion.

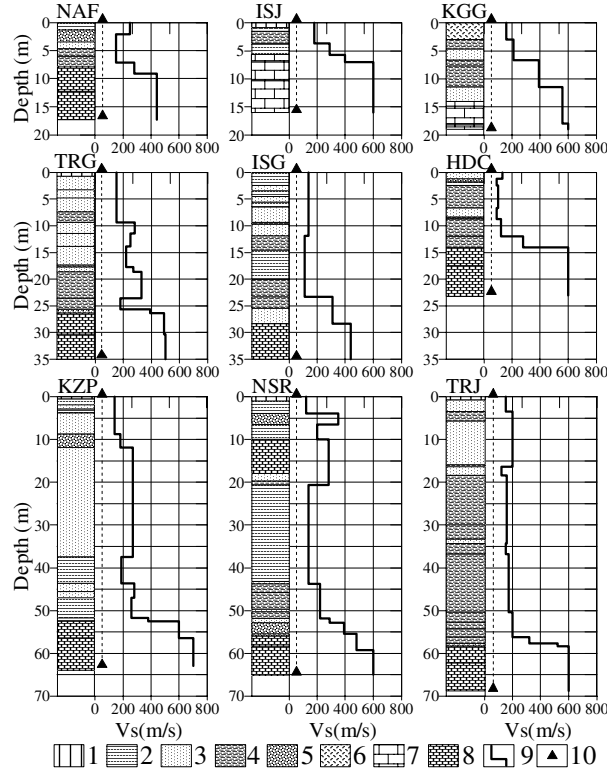


Figure 5. Soil- and S-wave velocity-profiles of the nine sites composing the vertical array. 1) Fill, 2) Silt, 3) Sand, 4) Clay, 5) Coarse Sand, 6) Loam, 7) Soft Rock, 8) Mudstone, 9) S-wave velocity, 10) Accelerographs

In order to check the magnitude of the influence of the vertical motion amplifications we calculated the empirical horizontal to vertical spectral ratios (H/V) employing the vertical array data according to the expression:

$$H/V(f) = \frac{G_H(f)}{G_V(f)} = \frac{H_S(f)/H_B(f)}{V_S(f)/V_B(f)} \quad (4)$$

where G_H and G_V denote the amplification spectrum calculated for the horizontal (H) and vertical (V) components of motion recorded at the surface (S) and base (B) layer accelerographs, respectively. We illustrate the results obtained from the implementation of this equation in Fig. 6 below.

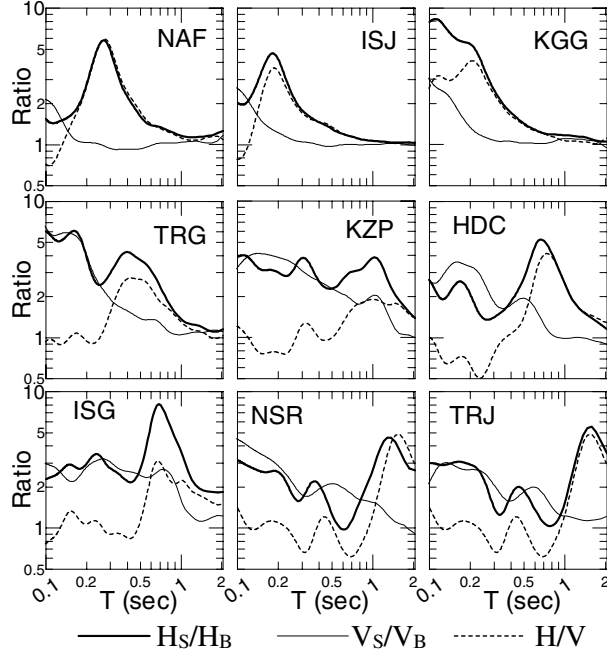


Figure 6. Comparison of the surface-to-borehole spectral ratios for the horizontal (H_S/H_B), and vertical (V_S/V_B) motion of S-waves, and the corresponding surface-to-borehole H/V ratio

Simultaneous comparison of all surface-to-borehole spectral ratios makes clear that the vertical component of motion does not undergo significant amplification at the resonance frequencies of the horizontal components of motion. At sites TRG and KZP, however, both components of motion undergo amplification in the short period part of the spectrum, and therefore, taking the ratio given by Eq. 4 abridges the amplification ratios. At this point, we find it worth clarifying that at sites TRG and KZP the resonance frequency for the first mode of vibration appears clearly defined in both amplification spectra: in the horizontal motion transfer function by a clear peak, and in the vertical motion transfer function by relatively low amplification, stable within a factor of two. In site effects studies, among all parameters under consideration, we pay particular attention to the predominant periods. Examination of Fig. 6, however, reveals that at TRG and KZP the predominant periods do not coincide with the resonance periods for the first mode of vibration, and appear located in the shorter period part of the spectrum. It turns apparent that in these cases the H/V ratio given by Eq. 4 provides both, inexact transfer functions, and biased predominant periods and maximum amplification ratios. Furthermore, although at the rest of the sites we obtain an overall good coincidence of predominant periods, we cannot state the same for the rest of the frequency range under consideration. The previous assertion applies even to sites NAF, ISJ, and TGG in the very short period part of the spectrum. At sites HDC, ISG, NSR, and TRJ, when compare with the surface to borehole transfer functions for the horizontal component of motion, the resulting H/V transfer functions display an obvious mismatch of spectral ratios at periods other than those related to the

predominant peaks. If we aim at assigning only predominant periods and maximum spectral ratios, then we can state that amplification of the vertical component of motion will not significantly affect the results as long as the H/V spectra display a prominent peak. We clarify this idea dividing the sites illustrated in Fig. 6 into three groups representing the general cases:

1) Sites NAF, ISJ, KGG: The horizontal motion transfer function (H_S/H_B) displays a clear main peak in the short period part of the spectrum. The vertical motion transfer function (V_S/V_B) remains essentially flat, displaying only relatively small amplification ratios at periods shorter than 0.2 seconds. Consequently, calculation of the H/V ratio, as given by Eq. 4, will provide good estimations of predominant periods, because, euphemistically speaking, “the predominant periods have no other place left to go”.

2) Sites HDC, ISG, NSR, and TRJ: The H_S/H_B transfer functions display more than one peak, with the predominant one located in the relatively long period part of the spectrum. The (V_S/V_B) transfer functions show that the vertical component undergoes amplification, with a clear tendency to display larger amplification ratios towards the short period part of the spectrum. Accordingly, calculation of the H/V ratio will not affect the assessment of the predominant periods, for cancellation of the peaks located in the short period portion of the spectrum do nothing but to enhance the predominant peaks, namely, the resonance periods for the first modes of vibration.

3) TRG and KZP: The H_S/H_B transfer functions indicate that the horizontal component of motion undergoes larger amplifications towards short periods. We can also observe a second peak indicating the resonance frequency for the first mode of vibration. This peak, however, does not “predominate” when compared to those at short periods. The (V_S/V_B) transfer functions indicate that the vertical components of motion undergo amplifications at short periods, following a trend similar to those obtained for the horizontal component. The vertical components, however, show no significant amplifications towards longer periods, particularly at those coinciding with the resonance peaks for the first mode of vibration. Therefore, taking the H/V ratio apparently cancels the short period peaks, thereby swaying the predominant peaks towards longer periods.

We can summarise the previous discussion stating that the H/V spectral ratio appears to provide good estimations of predominant periods under the following conditions:

- 1) Sites at which the vertical component of motion does not undergo significant amplifications
- 2) Sites at which the vertical component of motion:
 - i) Undergoes amplification along the frequency range under scrutiny, but
 - ii) Displays no significant amplification at the frequencies coinciding with the predominant peaks of the horizontal component, which coincide with the frequencies for the first modes of vibration (long periods)

We can state that if we consider all the frequency range under consideration, then we must admit that the H/V transfer functions underestimate the spectral ratios at frequencies other than the resonance ones. This turns even more conspicuous when basing the estimation of site effects on the H/V technique, for microtremor analysis does not succeed in revealing second and higher order resonance peaks. According to what we have seen so far, when estimating site effects using microtremors we face two main problems:

- 1) Conspicuous mismatches of predominant periods at sites characterised by a complex soil profile
- 2) Different levels of deviation from the H_S/H_R -based transfer functions along the frequency interval under consideration for frequencies other than those corresponding to the predominant periods.

We find noteworthy the similitude of the H/V amplification spectra calculated from the vertical array data and that of microtremors, even for sites characterised by mismatching H_S/H_R transfer functions, such as TRG and KZP. Thus, we can conjecture that these results, although based on the analysis of the S-wave portion of ground motion, should also apply to microtremor data. Apparently, our conjecture regarding the validity of these results for microtremors demands corroboration. To authenticate these results we need microtremor data simultaneously recorded on the surface and at boreholes, which we actually do not have. If we analyse closer the ground motion recordings, however, then we will realise that for some events the recordings start before the arrival of the P-waves. These portions correspond to

the so-called “noise”, or “background noise”. Faced with the absence of better microtremor data, however, we must consider whether we can treat these portions of the recordings as microtremors. This possibility appears closely related to the precision of the network. In other words, in order to obtain reliable results, the minimum amplitude of these minute ground motions preceding the arrival of the P-waves must surpass no less than ten times the precision of the recordings. When dealing with the coda waves’ portion of the recordings we corroborated that the Yokohama Strong Motion Network records ground motion with a precision of 3.8 miligals. Accordingly, we can state that we can use these data to calculate the surface to borehole spectral ratios of microtremors without significantly compromising the quality of the results.

In order to corroborate the validity of the results obtained for the S-wave portion of ground motion in the case of microtremors, we calculated both, the horizontal (H_N/H_B) and vertical (V_N/V_B) components amplification spectra, and applied Eq. 4 to obtain a “true” H/V ratio of microtremors from the borehole data. The resulting amplification spectra plotted in Fig. 7 display a remarkable coincidence with those obtained from the analysis of ground motion (Fig. 6). This appears to confirm the validity of the conclusions we derived from the analysis of ground motion for the case of microtremors as well.

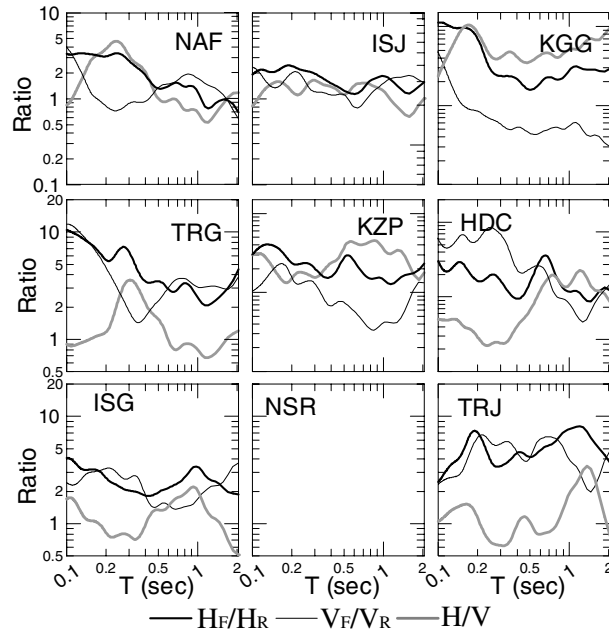


Figure 7. Comparison of the surface-to-borehole spectral ratios for the horizontal (H_N/H_B), and vertical (V_N/V_B) motion of microtremors, and the corresponding surface-to-borehole H/V ratio

VALIDATION OF THE ROBUSTNESS OF THE SPECTRAL AMPLIFICATION PATTERNS THROUGH THEORETICAL CALCULATIONS

We begin examining the correspondence of empirical and theoretical transfer functions by focussing on the analogies of the empirical transfer functions with the SH transfer functions for vertically incident SH waves computed in compliance with the Thompson-Haskell method [4, 5] at the vertical array sites. Figure 8 illustrates H_S/H_R , H/V_M , and SH transfer functions obtained for the S-wave velocity profiles typical for the nine patterns plotted in Fig. 4. Examination of the plots shows that the grouping scheme derived from the application of cluster analysis also discloses a coherent sequence of theoretical SH transfer functions. The results show that at Pattern I sites the SH transfer functions display better agreement with the H_S/H_R spectral ratios than with the H/V_M ones. Moreover, we can state that at sites pertaining to Pattern I, the H/V_M amplification spectra cancel the peaks located in the short period part of

the spectrum. The SH transfer functions, however, confirm that at Pattern I sites the soil profiles induce significant amplification of S-waves in the short period part of the spectrum. On these grounds, we can indubitably state that the H/V_M method provides biased soil response estimations at sites characterised by soil profiles as those pertaining to Pattern I sites (Figs. 12 and 4). The good agreement of the empirical H_S/H_R and H/V_M amplification spectra with the theoretical SH transfer functions for the sites composing the remaining eight patterns also confirm the robustness of the adopted grouping scheme.

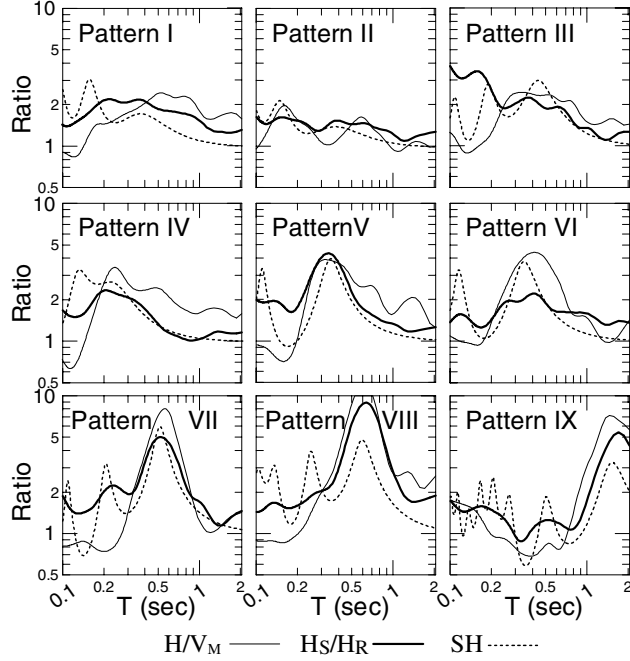


Figure 8. The matching of empirical and theoretical transfer functions for each pattern. The transfer functions correspond to sites characterised by the typical S-wave velocity profiles plotted in Fig. 4.

However, it turns difficult to comprehend why the H/V_M, a technique whose application relies on the Rayleigh wave content of microtremors, provides good results when applied to the more energetic S-wave portion of ground motion. We further verify the applicability of the H/V spectral ratio through numerical modelling of the source of excitation as harmonic plane S-waves [4, 6]. Let's assume that site effects arise as result of the filtering induced by a layer overlaying a half-space. The vertical motion admits non-zero values only if we consider SV plane waves with an angle of incidence different from vertical. The parameters of the calculation model comprise the angle of incidence, the geomechanical properties of the layers composing the soil profile, and their corresponding thickness, which operates as a scaling factor for the frequency axis. The procedure usually applied comprises the estimation of the soil transfer function as the ratio of the amplitude of the horizontal motion ($U_S(f)$) with respect to the amplitude of the incident wave at the base of the sedimentary package ($U_{SH}(f)$).

$$U_S(f)/U_{SH}(f) \quad (5)$$

Similarly, we can estimate the soil transfer function for the vertical motion by taking the ratio of the amplitude of the vertical motion ($W_S(f)$) with respect to that of the incident wave ($U_{SH}(f)$):

$$W_S(f)/U_{SH}(f) \quad (6)$$

Apparently, if the source of excitation remains constant, the transfer functions vary proportionally to the angle of incidence γ measured from the vertical by a factor $\cos(\gamma)$. According to these definitions, the horizontal to vertical spectral ratio constitutes an estimation of site effects only if the ratio given by Eq. 6 equates unity:

$$\frac{U_s(f)/U_{SH}(f)}{W_s(f)/U_{SH}(f)} = \frac{U_s(f)}{U_{SH}(f)} \text{ only if } \frac{W_s(f)}{U_{SH}(f)} \geq 1 \quad (7)$$

We implemented Eqs. 5, 6, and 7 to compute the transfer functions within the frequency interval 5~10 Hz (0.1~2 sec) for consecutive increments of 1° in the angle of incidence, up to 70° . Figure 9 illustrates the results for the soil profile at site HDC (Fig. 5). The plot on the left represents the normalised amplification spectrum for the horizontal motion, the middle plot that for the vertical motion, while the right side plot represents the theoretical horizontal to vertical ratio, namely, the theoretical H/V ratio. Examination of these plots appears to indicate that the vertical motion undergoes a rather negligible amplification along the whole frequency range under scrutiny. We can also state that the amplification of the vertical component remains within a factor of two for angles of incidence smaller than the critical angle. Furthermore, the vertical motion amplification displays clear troughs at the resonance peaks of the horizontal components of motion. As we can observe, the theoretical H/V transfer functions display very good agreement with the empirical ones, as long as we do not surpass the critical angle of incidence, in this case about 20° .

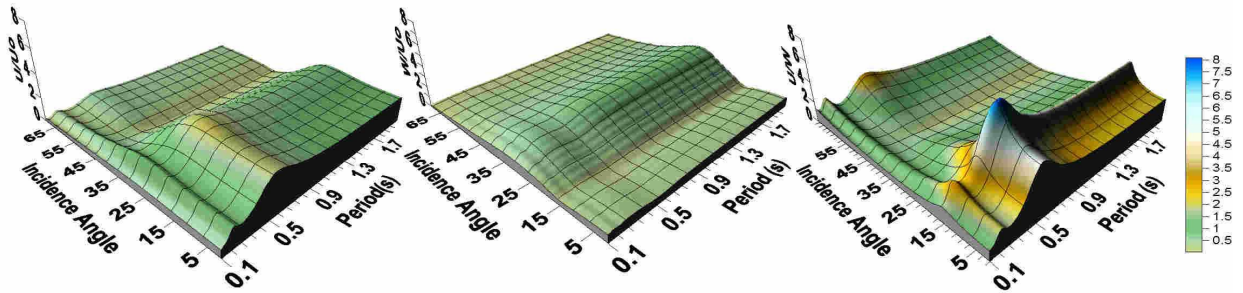


Figure 9. Theoretical soil response functions for incident SV plane waves. U: Amplitude on the horizontal component of motion, W: Amplitude on the vertical component of motion, Uo: Amplitude of the incident wave, U/W: Theoretical H/V spectral ratio.

We illustrate similar H/V theoretical transfer functions for the nine sites composing the vertical array in Fig. 10. As we can observe, calculation of the H/V ratio at sites other than TRG and KZP results in enhancement of the resonance peaks of the horizontal components. At sites TRG and KZP, however, the H/V ratio apparently reduces the magnitude of the short period peaks. This also appears to coincide with the empirical transfer functions obtained for these two sites, as shown in Figs. 6, 7, and 8.

After analysing Fig. 10, we can say that, on one hand, the theoretical calculation of H/V ratios using one-dimensional methods proves the applicability of the H/V technique even to the S-wave portion of ground motion. On the other hand, we can state that the drop of the theoretical H/V ratios indicates that the H/V technique fails to reveal the true amplification in the short period part of the spectrum at sites characterised by complex soil profiles (Fig. 5, TRG and KZP). Accordingly, the numerical calculations corroborate the results obtained from the application of empirical methods and the robustness of the adopted grouping scheme.

SPECTRAL AMPLIFICATION PATTERNS FOR SITE CLASSIFICATION (PROPOSITION OF THE SAP METHODOLOGY)

The methods most often employed in seismic zonation and microzonation studies on site effects rely on purely empirical formulas, or empirically derived relations linking certain ground motion parameters with the local geology. These methods usually rely on the statistical analysis of microseismic information in conjunction with geological and geomorphological maps. Surface geology maps, although informative, do not provide information to estimate the effect of the soil profile on ground motion with the required

accuracy, for they appear as a rather poor representation of the soil profile at depth, namely, the third geological dimension. As suggested by theoretical studies, we can treat the propagation of seismic waves in layered media as a one-dimensional problem involving reflections and refractions along the vertical (x , z) plane. Accordingly, it seems obvious that site amplification arises as a phenomenon mostly related to the vertical plane. In other words, geological maps reflect the spatial distribution of the geological units within the territory under study in the horizontal, but not in the vertical plane. When we employ microtremors, we aim at discretising the spatial distribution on the horizontal plane of the influence of the vertical plane, namely, the influence of the soil profile as the third geological dimension. In this regard, to plot only reliable values of the parameters under analysis and extrapolate them to sites characterised by unreliable estimations relying on the similitude of the surface geology appears to do nothing but to worsen the results. In other words, we cannot assign reliable site-specific parameters relying on the characteristics of the surface geology, simply because surface geology maps do not reflect the distribution of the soil layers at depth. This seems to limit the usefulness of formulas and methods based on procedures linking site effects with the surface geology.

We may cite, for example, that we may calculate a response spectrum employing the coefficients recommended for “rock” or “soil” ground, but how do we classify a site as rock or soft soil relying only on the information provided by a surface geology map? The application of this procedure within Yokohama City, for example, leaves no alternative but to classify most of the sites as soft soil sites. In the course of our study, however, we confirmed that sites located on the same geological units often appear characterised by completely different soil profiles and contrasting amplification spectra. Furthermore, the usefulness of surface geology maps appears to bear an inversely proportional relation with the mapping scale, for their usefulness decreases as we move toward more detail studies. This assertion stands on the fact that detail site effects studies require information on the subsurface geology, which surface geology maps usually lack.

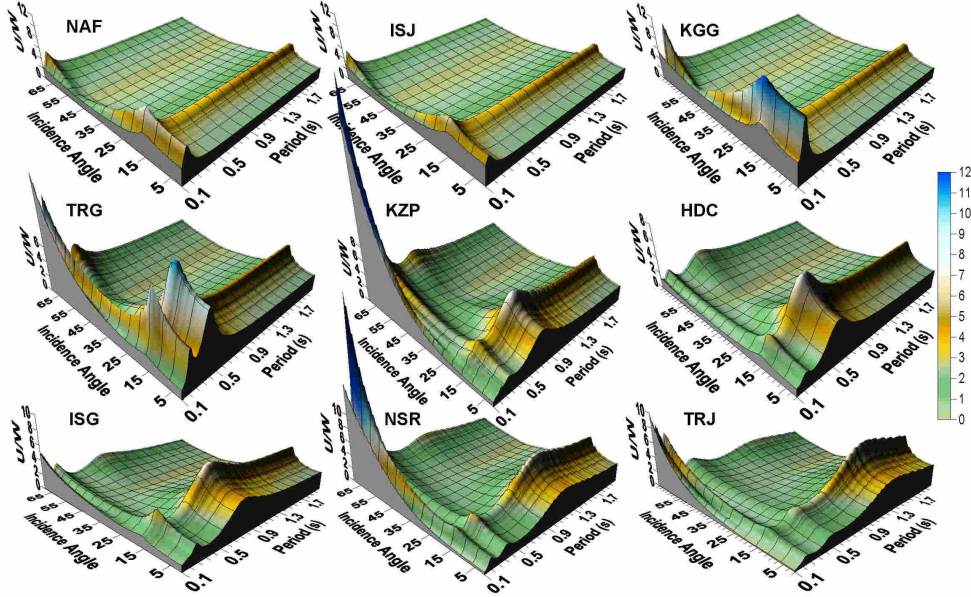


Figure 10. Theoretical H/V soil response functions for incident SV plane waves.

It seems worth clarifying that surface geology maps do not provide misleading or erroneous data. On the contrary, when combined with other geological and geophysical data, a surface geology map may help clarifying a whole range of unknown issues within our target area. Broad classifications based on the surface geology, however, arise as consequence of a multiplicity of constraints imposed by the lack of detailed information. We often feel tempted to solve this problem assuming that we can rely on the

surface geology to judge the magnitude of site effects on ground motion. Accordingly, when the results themselves do not match reality (and our expectations as well), we can but to say that our assumptions regarding the surface geology, not the surface geology maps, led to erroneous results. Our results corroborate that the H/V technique does incur clear mismatches at sites characterised by the complexity of their soil profiles. From the practical point of view, this seems to seriously hinder the reliability of microtremor-based estimations, thereby limiting the applicability of the method. Our approach to improve the effectiveness of the H/V technique comprises using the knowledge we have acquired so far on the category structure of the H_S/H_R vs. H/V_M amplification spectra.

We can treat the average mismatch with respect to the H_S/H_R -based transfer functions as the general tendency permeating the microtremor-based estimations. When dealing with the amplification spectra for the sites composing the nine Spectral Amplification Patterns determined in our study, the task turns relatively easy, because counting with both, the soil profile, and the corresponding soil response given by the H_S/H_R transfer functions allows expeditious cross-validation of the H/V_M spectra. The assessment of the reliability of H/V_M -based site effects estimations when counting with no other data but microtremors, however, arises as a particularly difficult task. Yet, when attempting to expand the applicability of microtremors in site effects studies, the assessment of this reliability turns into an unavoidable problem. Summarising the results we have obtained so far, we can mention the following issues:

- 1) The Spectral Amplification Patterns attained in our study display similar H/V_M and H_S/H_R amplification spectra
- 2) We can consider the shape of the H/V_M spectra characterising each pattern as concomitant with specific soil profiles
- 3) These nine dual spectral patterns appear characterised by varying levels of coincidence of estimations, with Pattern I sites characterised by complex soil profiles and the worst coincidence of amplification spectra

We can apply these inferences to assess the reliability of the H/V_M estimations relying only on H/V_M amplification spectra. Here, we also find worth pointing out that site effects studies target the estimation of the parameters characterising the soil response to a dynamic load, in this case earthquake ground motion. Accordingly, no matter the method employed, we always target the estimation of the transfer functions characterising the effects of the soil profile on ground motion. The use of microtremors constitutes no exception, for our interest in microtremors originates from the possibility of using microtremor analysis as the vehicle to estimate the magnitude of site effects on ground motion. The level of coincidence between H/V_M and H_S/H_R transfer functions appears related to the characteristics of the soil profile. Furthermore, considering the level of similarity of both amplification spectra we divided our dataset into nine groups representing the category structure of their mutual relationship. We denominated these groups as Spectral Amplification Patterns, for their member sites appear robust not only in terms of coincidence of amplification spectra, but also in terms of similitude of their soil profiles and spatial distribution.

On the light of these results, we can treat the shape of the H/V_M amplification spectra as concomitant with similar characteristics of the soil profile. This in turn opens the possibility of using the H/V_M spectra to identify the general characteristics of the soil profile through comparison with the mean H/V_M transfer functions characterising the nine Spectral Amplification Patterns. Once we identify the new sites as members of one of the nine SAPs, we can evaluate the reliability of the H/V_M spectra relying on the H_S/H_R transfer functions for each particular pattern. Once evaluated, we can employ the general mismatching tendency of the H/V_M with respect to the H_S/H_R to detrend the H/V_M estimations and assign more reliable site effects parameters. Thus assigned, these parameters will still preserve the desired site-specific characteristics, for their assignment relies on detrending microtremor-based spectra calculated for each particular site. In a nutshell: we can employ the H/V_M spectral shapes as indicators of the general characteristics of the soil profile at each particular site, and with the aid of the SAPs we can in turn judge their reliability and detrend those providing biased estimations. To detrend the H/V_M -based amplification spectra, we first calculate the general mismatching trend permeating each of the patterns as a series of

coefficients given by the following expression:

$$B(f) = H_S/H_R(f) / H/V_M(f) \quad (8)$$

where (B) represents the series of coefficients given by the ratio of the H_S/H_R values to the H/V_M ones along the frequency interval (f) under analysis.

According to this definition, we can consider the resulting $B(f)$ series of coefficients representing the general trend of the biases as “detrending spectra”. It turns apparent that we can attempt to detrend the microtremor-based estimations by multiplying the corresponding H/V_M amplification spectra by these coefficients, namely:

$$H/V_{DM}(f) = H/V_M(f) * B(f) \quad (9)$$

Consideration of the afore-mentioned issues led us to conclude that we can utilise Spectral Amplification Patterns to improve the efficacy of microtremor analysis in site effects studies. Accordingly, we proceeded to propose a new methodology for the estimation of site effects based on the use of Spectral Amplification Patterns for H/V_M spectral ratios. The resulting site classification scheme comprises three main stages:

(I) Calculation of the H/V_M Amplification Spectra and Determination of Predominant periods and Maximum Spectral Ratios:

We use plural to emphasise the idea of evaluating a set of microtremor-based amplification spectra rather than isolated cases. Once we estimate the corresponding predominant periods and maximum spectral ratios, we compare them with those characterising the Spectral Amplification Patterns using the plot illustrated in Fig. 11. This provides a relatively fast procedure to evaluate the reliability of the H/V_M -based parameters.

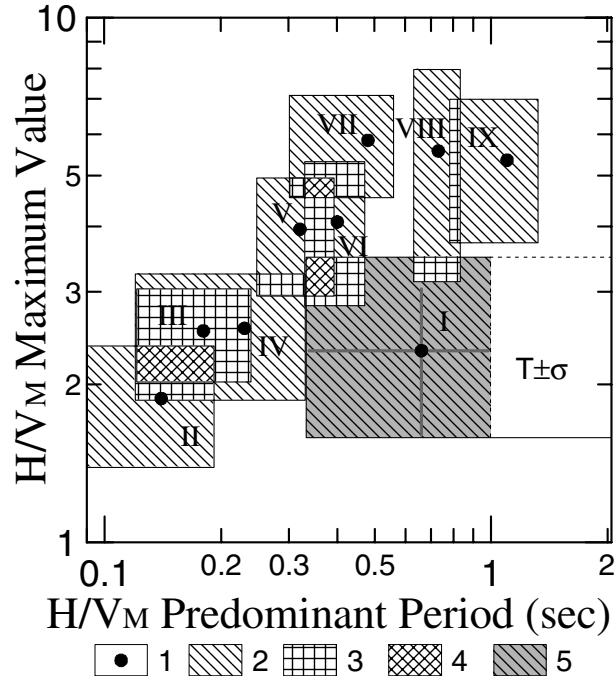


Figure 11. Plot recommended for the preliminary evaluation of the reliability of H/V_M -based site effects' estimations. The rectangular areas represent the regions of influence ($\pm\sigma$ of the average predominant periods and maximum spectral ratios) for the nine Spectral Amplification Patterns (SAP). 1: Average values for each pattern, 2: No overlapping of regions, 3: Two regions overlap, 4: Three regions overlap, 5: Pattern I region. When the values fall on overlapped regions, in order to evaluate the reliability of the H/V_M -based parameters we must check the matching of the new H/V_M overall spectral shape with those for the SAP illustrated in Fig. 12.

If the parameters for the sites undergoing evaluation plot within the grey region around Pattern I, then we must evaluate the site with extreme care, for most probably the H/V_M spectra appears biased by the influence of a complex soil profile.

II) Evaluation of the H/V_M Reliability:

In this stage, we compare the spectral shape of the H/V_M spectra calculated in Step I with those corresponding to the nine Spectral Amplification Patterns. In short, we classify the sites under analysis as a member of one of the nine categories represented by the SAPs illustrated in Fig. 12. As similar H/V_M spectral shapes appear concomitant of similar soil profiles, once classified, we may extrapolate the reliability of the H/V_M for each pattern to the new member sites.

III) Assessment of Site Effects Parameters:

Once we identified the sites membership to one of the patterns, we can then use the tendency of the mismatch typical for each pattern to detrend the H/V_M spectra using the series of coefficients (B) given by the spectra represented with a dot line in Fig. 12.

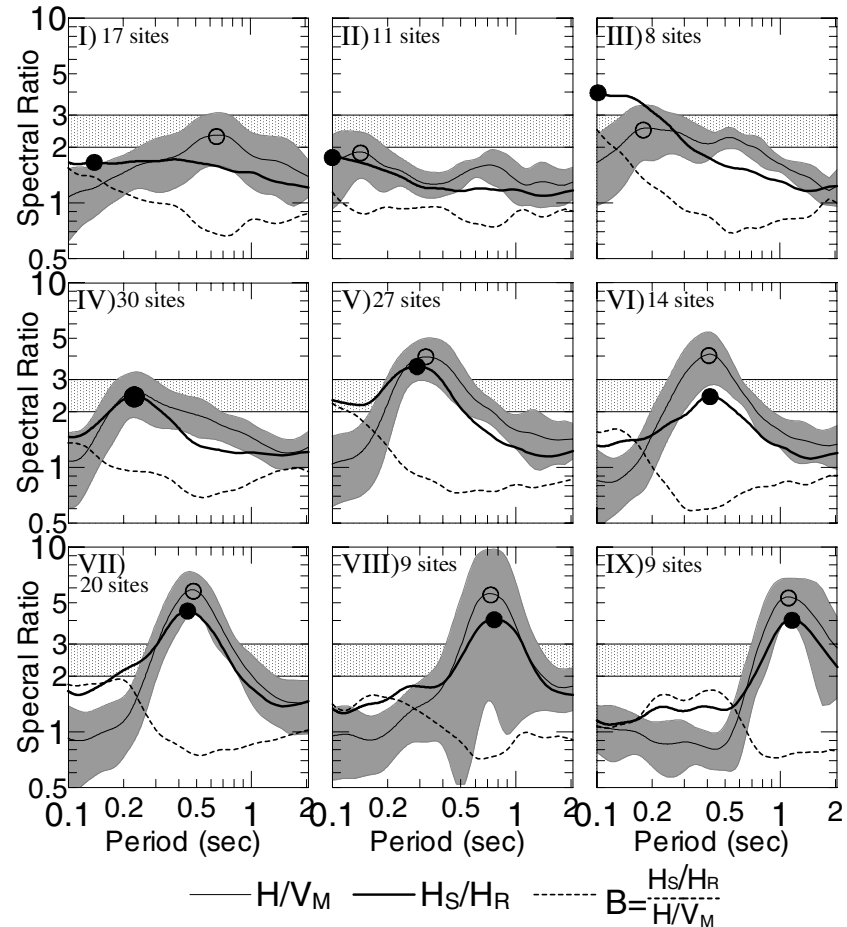


Figure. 12. Plot intended for closer examination of the matching between new H/V_M spectra and the overall shape of the average H/V_M spectra characterising the nine Spectral Amplification Patterns (SAP). The grey shaded area represents the $H/V_M \pm \sigma$ region. Once identified, we can obtain the detrended H/V_{MD} spectra through multiplication by the series of correction factors indicated by the dotted spectra, namely: $H/V_{MD} = H/V_M * B$. In the case of dealing with Pattern-I sites detrending turns customary. In the rest of the cases, we also recommend detrending, for this operation appears to provide better-behaved maximum amplification ratios. Application of this detrending procedure in cases other than Pattern I sites, however, turns into a matter of personal judgement. Once we complied with this procedure, we

can assess the final site effects' parameters from the detrended (DM) H/V_{MD} spectra.

The SAP Method thus defined postulates the possibility of identifying biased H/V_M amplification spectra through visual (or computer aided) comparison with the mean H/V_M spectra typical of the nine Spectral Amplification Patterns. We can also apply less subjective methods, such as employing these nine patterns as training sample in a supervised pattern recognition process. The use of spectral amplification patterns as the basis of the comparison allows us to classify the identification of possibly biased H/V_M estimations as "an educated guess". Once we identified biased H/V_M amplification spectra, the next step consists in using the mean H_S/H_R and H/V_M amplification spectra to remove the bias.

CONCLUSIONS

In this study, the authors applied a pattern recognition approach to identify the general trends and common features accompanying both, success and failure of the H/V technique and their relation with the local geological conditions. The grouping scheme thus derived led to the proposition of concrete guidelines targeting the improvement of the accuracy and reliability of microtremors in site effects estimations. From the results we can conclude the following:

- 1) We can organise the sites composing the Yokohama Strong motion Network in relatively homogeneous groups of sites relying on the corresponding H_S/H_R and H/V_M coincidence level. The nine patterns thus defined represent a category structure that fits their mutual relationship.
- 2) Analysis of the soil profile and the spatial distribution of the sites composing these nine patterns appear to confirm the robustness of the partitioning process. This in turn suggests the possibility of assessing the reliability of H/V_M estimations relying on the use of Spectral Amplification Patterns (SAP).
- 3) Pattern I sites appear characterised by conspicuously large overestimations of predominant periods when using the H/V_M technique as estimation tool. Therefore, expansion of the applicability of microtremors analysis depends heavily on the correction of the estimations at Pattern I-like sites.

In order to further check the validity of the transfer functions, as well as the validity of the spectral patterns resulting from the pattern recognition process, we applied theoretical one-dimensional (1D) analysis using the available logging data, and calculated surface to borehole spectral ratios for the horizontal and vertical components of motion (S-waves and microtremors) at the vertical array sites. The results indicate the following:

- 4) Analysis of the transfer functions for vertically incident SH plane waves after organising the sites into nine categories confirms that the H/V_M technique incur clear overestimations of predominant periods at Pattern I sites. Moreover, the similarity of the SH transfer functions for the sites composing each pattern confirms the robustness of the adopted grouping scheme.
- 5) Calculation of surface to borehole spectral ratios for the vertical components of motion indicates that the vertical components undergo amplification for frequencies higher than five hertz even at sites characterised by a relatively simple soil profile. At sites characterised by a more complex soil profile the vertical components of motion undergo relatively small amplifications at other frequencies too. At the resonance frequencies of the horizontal components, however, the vertical components of motion do not undergo but negligible amplifications. These results appear to substantiate the assumption that we can treat the ground motions recorded by the vertical components of the surface accelerographs as representative of the source. This in turn seems to validate the use of the vertical components at the surface as representative of the incident waves arriving at the base of the sedimentary packages. Notwithstanding, amplification of the vertical component at different frequencies, although relatively small, will obviously sway the corresponding H/V amplification spectra away from the transfer functions for the horizontal component of motion.
- 6) The H/V spectral ratio technique appears to provide good estimations of predominant periods under two conditions:

- a) Sites at which the vertical component of motion does not undergo significant amplifications,
 - b) Sites at which the vertical component of motion does undergo amplification along the frequency range under scrutiny, but displays no significant amplification at the frequencies coinciding with the predominant peaks of the horizontal component. These peaks usually coincide with the frequencies for the first modes of vibration (toward long periods).
- 7) We confirmed that, if we consider all the frequency range under consideration, then we must admit that the H/V transfer functions underestimate the spectral ratios at frequencies other than the resonance ones. This seems even more conspicuous when basing the estimation of site conditions on the H/V_M technique, for microtremor analysis does not succeed in revealing second and higher order resonance peaks.
- 8) Examination of theoretical transfer functions for SV waves incident at different angles at the base of the sedimentary packages appears to confirm that the vertical motion undergoes a rather negligible amplification along the whole frequency range under scrutiny. We can also state that the amplification of the vertical components remains within a factor of two for angles of incidence smaller than the critical angle.
- 9) The vertical motion for SV plane waves displays clear troughs at the resonance peaks of the horizontal components of motion. This results in the enhancement of the resonance peaks of the horizontal components when taking the H/V ratio. At sites TRG and KZP, however, the H/V thus obtained apparently reduces the values of the short period peaks. This result coincides with the empirical transfer functions obtained for these two sites.
- 10) The theoretical calculation of H/V ratios using one-dimensional methods proves the applicability of the technique even to the S-wave portion of ground motion. The relative reduction of the magnitude of the peaks in the short period part of the spectrum for sites characterised by a complex soil profile, however, appear to indicate that the H/V technique fails to reveal the true amplification ratios in the short period part of the spectrum at sites characterised by a complex soil profile.
- 11) The results attained from the calculation of surface to borehole spectral ratios for both, ground motion and microtremor data indicate that when estimating site effects using microtremors we face two main problems: a) Conspicuous mismatches of predominant periods at sites characterised by a complex soil profile, and b) Different levels of deviation from the H_S/H_R -based transfer functions along the frequency interval under consideration at frequencies other than those coinciding with the predominant ones.
- 12) Based on these results, we postulated the use of Spectral Amplification Patterns (SAP) to improve the accuracy of the H/V_M -based estimations. The SAP Method thus defined relies on the fact that mismatching H/V_M amplification spectra display a trend that repeats at sites characterised by a similar soil profile, and thus, we can treat it as a bias. Accordingly, the use of Spectral Amplification Patterns permits to identify mismatching H/V_M spectra and link them to potentially complex soil profiles. This in turn makes possible to use the general mismatching trend typical of each particular pattern to detrend the microtremor-based estimations. The detrended H/V_M amplification spectra thus corrected show a much better agreement with H_S/H_R transfer functions and their corresponding predominant periods and maximum amplification ratios.
- 13) The SAP Method presents the possibility of evaluating the reliability of microtremor-based estimations of site effects relying solely on microtremor measurements. When integrated into a robust set of Spectral Amplification Patterns, as the ones proposed in our study, we can employ even mismatching H/V_M spectra to identify the general characteristics of the sites' soil profile, as well as to assign more reliable site effects parameters relying on their H_S/H_R counterparts. Accordingly, the attainment of Spectral Amplification Patterns makes a reality the employment of microtremors as a tool to investigate the most influential, and at the same time most impalpable factor influencing ground motion: the composition of the soil profile as the third (vertical) geological dimension, namely, the subsurface geology. This turns a reality because the amplification spectra for each of the nine patterns postulated in our study represent the result of the influence of soil profiles with distinguishable

characteristics of their own. Apparently, the possibility of classifying the sites into nine categories relying on microtremors allows a more realistic and accurate assessment of both, the sites effects, and the characteristics of the soil profile than classifications and empirical formulas that rely on the surface geology.

14) Extension of this methodology to the H/V spectral ratio of S-waves and the Coda portions of ground motions appears straightforward. Furthermore, the attainment of Spectral Amplification Patterns relating transfer functions obtained from the application of better-understood methodologies and techniques still not so well understood appears to provide an alternative to improve their reliability and applicability while we fill the gap in our theoretical understanding of some techniques. In other words, as long as we find ways to improve their accuracy and reliability, our lack of purely theoretical understanding of a technique should not become an obstacle to its applicability, for ultimately they must serve a practical engineering purpose.

ACKNOWLEDGEMENTS

This study became possible under the auspices of a scholarship granted by the Japanese Ministry of Education. Hereby, we express our deepest gratitude to the people of Japan for making such opportunities available.

REFERENCES

1. Rodríguez V.H.S. and Midorikawa S., 'Applicability of microtremors in assessing site effects on ground motion', *Earthquake Engineering & Structural Dynamics*, 31, 261-279, 2002
2. Rodríguez V.H.S. and Midorikawa S., 'Comparison of Spectral Ratio Techniques for Estimation of Site Effects using Microtremor Data and Earthquake Motions recorded at the Surface and in Boreholes', *Earthquake Engineering & Structural Dynamics*, 32, 1691-1714, 2003
3. Borcherdt R. D., 'Effects of Local Geology on Ground Motion near San Francisco Bay', *Bull. Seis. Soc. Am.* 60, 29-61, 1970
4. Haskell, N.A., 'The dispersion of surface waves in multilayered media', *Bull. Seis. Soc. Am.*, 43, 17-34, 1953
5. Fukushima Y. and Midorikawa S., 'Evaluation of site amplification factors based on average characteristics of frequency dependent Q^{-1} of sediment strata', *Jour. Constr. Eng., AIJ*, 460, 37-46, 1994 (in Japanese)
6. Lermo L. and Chaves-García J., 'Site effect evaluation using spectral ratios with only one station', *Bull. Seis. Soc. Am.* 83-5, 1574-1594, 1993